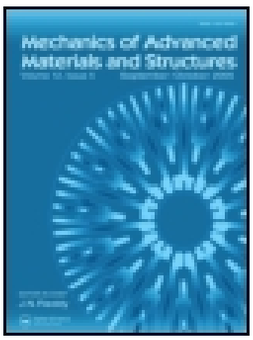

Mechanics of Advanced Materials and Structures

ISSN: 1537-6494 (Print) 1537-6532 (Online) Journal homepage: http://www.tandfonline.com/loi/umcm20

The effects of strength models in numerical study of metal plate destruction by contact explosive charge

Tuan Truong Anh, Thom Do Van, Dat Pham Tien & Nguyen Dinh Duc

To cite this article: Tuan Truong Anh, Thom Do Van, Dat Pham Tien & Nguyen Dinh Duc (2018): The effects of strength models in numerical study of metal plate destruction by contact explosive charge, Mechanics of Advanced Materials and Structures, DOI: 10.1080/15376494.2017.1410907

To link to this article: https://doi.org/10.1080/15376494.2017.1410907

MECHANICS OF ADVANCED MATERIALS AND STRUCTURES
2017, VOL. 0, NO. 0, 1–10
https://doi.org/10.1080/15376494.2017.1410907

Taylor & Francis
Taylor & Francis Group

ORIGINAL ARTICLE

The effects of strength models in numerical study of metal plate destruction by contact explosive charge

Tuan Truong Anh[a], Thom Do Van[a], Dat Pham Tien[a], and Nguyen Dinh Duc[b,c]

[a]Department of Weapon and Mechanics, Le Quy Don Technical University, Hanoi, Vietnam; [b]Advanced Materials and Structures Laboratory, VNU Hanoi – University of Engineering and Technology, Cau Giay, Hanoi, Vietnam; [c]Infrastructure Engineering Program, VNU Hanoi – Vietnam Japan University, Tu Liem, Hanoi, Vietnam

ABSTRACT

Based on a complete mathematical model, the authors set up a problem of metal plate destruction by contacting explosive charge in highly nonlinear dynamic software AUTODYN and solved in two cases using the Johnson–Cook and von Mises strength models. The numerical simulation results were compared with the experimental results and showed a good fit of numerical calculations versus experiments by using the von Mises strength model. The study also shows that the Johnson–Cook strength model, if applied unreasonably, will lead to large errors, which would help to avoid mistakes in the future high speed impact study.

ARTICLE HISTORY
Received 10 June 2017
Accepted 30 September 2017

KEYWORDS
Destruction; strength model; Johnson–Cook; von Mises; metal plate; contact explosive charge

1. Introduction

Destruction of the sheet and metal shell by contacting explosive charge is a problem in the field of high speed impact, which has been studied experimentally long time ago. Recently, thanks to the development of computer speed and software technology, these problems have begun to be solved by numerical methods.

In [1], the numerical setup of the fully coupled Euler–Lagrange simulations in two dimensions (fluid–structure interaction) with good results is shown. The TNT explosive (using the JWL equation of state) and the air (using the ideal gas equation of state) are modeled in the Eulerian part and the metal plate (using the Mie–Gruneisen equation of state) is modeled in the Lagrangian part. In order to check the applicability of the two-dimensional (2D) approach, a 3D model has been developed. In general, the physics of the process investigated can be described more accurately in three dimensions, but the resolution of the meshes cannot be chosen as fine as in 2D due to the high computational effort in 3D. In necessary case, in order to improve the speed and accuracy of the solution, the explosive load was measured experimentally and then placed on the structural surface by using the finite element code EUROPLEXUS with the advent of erosion criteria [2]. Except for special cases where materials are considered under the ultra-high stress level, which can be calculated using hydrodynamic codes, most practical applications must take into account the effects of strength to obtain a realistic solution [3].

Early studies of Hollomon, Ludwik, and Swift show a significant dependence of true stress on the true strain through the strain hardening exponent (n-value) [4]–[6]. Later, more perfect strength models have been proposed [7]: Johnson–Cook model the strength behavior of materials subjected to large strains, high strain rates and high temperatures; Zerilli–Armstrong in an approach seeking to improve the Johnson–Cook model proposed that each material structure type (fcc, bcc, and hcp) will have its own constitutive behavior, depending on the dislocation characteristics for that particular structure; Steinberg–Guinan have produced expressions for the shear modulus and yield strength as functions of effective plastic strain, pressure and internal energy (temperature) and constants for 14 metals.

In the Johnson–Cook strength model, the dynamic yield stress Y_d depends on the intensity of the plastic strain, the plastic strain rate, and the temperature as follows [8]–[10]:

$$Y_d = \left[A + B \cdot \left(\varepsilon_i^p\right)^n\right]\left(1 + C \ln e_{i0}^p\right)\left(1 - \bar{T}^m\right), \qquad (1)$$

where
A, B, C, n, m – experimental constants;
$e_{i0}^p = \frac{e_i^p}{\dot{\varepsilon}_0}$ – effective plastic strain rate when $\dot{\varepsilon}_0 = 1\ \mathrm{s}^{-1}$;
$\bar{T} = \frac{T - T_{room}}{T_{melt} - T_{room}}$ – homologous temperature;
T – temperature (K);
T_{room} – room temperature (K);
T_{melt} – melting temperature (K).

The Johnson–Cook model is widely used to describe the stress and deformation behavior under various loading conditions. However, with the Johnson–Cook model for each material sample, we have to determine the five experimental constants A, B, C, m, and n in the high strain rates range with highly specialized equipment [11]–[14], which are currently not available in many laboratories.

In the approximate case, some studies now use the experimental constants of the same material, but the margin of error is rarely sufficiently evaluated.

CONTACT Nguyen Dinh Duc ducnd@vnu.edu.vn Advanced Materials and Structures Laboratory, VNU Hanoi – University of Engineering and Technology, Cau Giay, Hanoi, Vietnam.
Color versions of one or more figures in this article are available online at www.tandfonline.com/umcm.

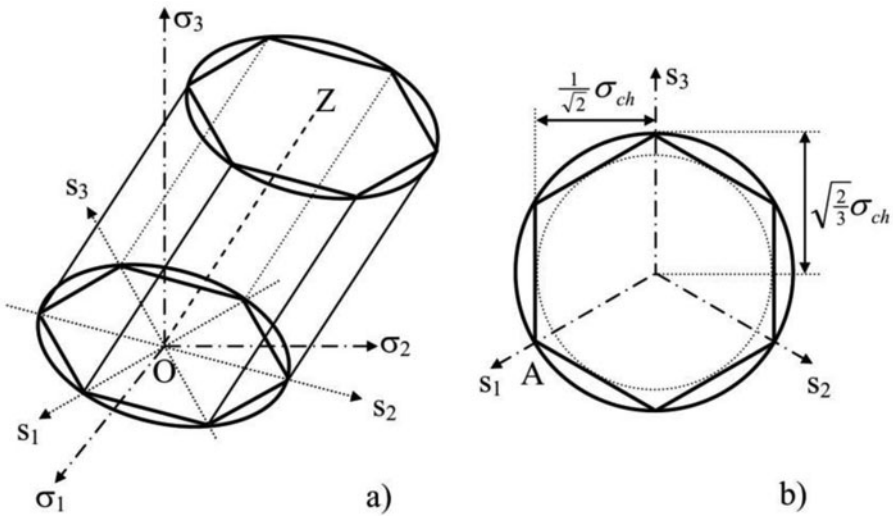

Figure 1. von Mises yield surface.

Unlike the Johnson–Cook model, the von Mises strength model has to determinate only the static yield stress value in simple tension test Y_s according to the following expression

$$(\sigma_1 - \sigma_2)^2 + (\sigma_2 - \sigma_3)^2 + (\sigma_3 - \sigma_1)^2 = 2Y_s^2. \quad (2)$$

Figure 1 describes the cylindrical yield surface in the principal stresses space $\sigma_1, \sigma_2, \sigma_3$ with radius

$$R = \sqrt{\frac{2}{3}} Y_s. \quad (3)$$

States lying inside the cylinder are elastic. States on the surface of the cylinder are plastic. Because of without taking into account the effects of strain hardening, strain rate or thermal softening (the static yield stress Y_s is kept constant throughout), the von Mises model was originally used to simulate quasi-static elastic–plastic flow [15]–[17]. However, a dynamic enhancement factor of 2 was used very successfully by Wilkins for simulating metal cylinder tests [18].

Research of the behavior of structures under intricate loadings (blast loading, impact loading, etc.) is very important since they play a necessary role in reality, especially in a war place like Afghanistan, Syria, etc. We have some published papers [18], [19], [21]–[27] to explore this problem, but these works only study structures in the field of elastic without experiment because of the high cost; this research follows the works before to find out the behaviors of structure in the field of plastic with experiment to show the accuracy of the theory model.

In this paper, the authors investigated the effects of von Mises and Johnson–Cook strength models on the value of error in numerical simulation of metal sheet destruction by contact explosive charge. The results obtained are the basis for choosing the strength model with the appropriate accuracy but more simple and convenient in material identification.

2. Mathematical model

The physical model of the interaction problem between the explosive and the steel plate is shown in Figure 2. We consider the explosive block (1) in a cylindrical form, flattened at the two ends, with diameter d and height L, placed in contact with

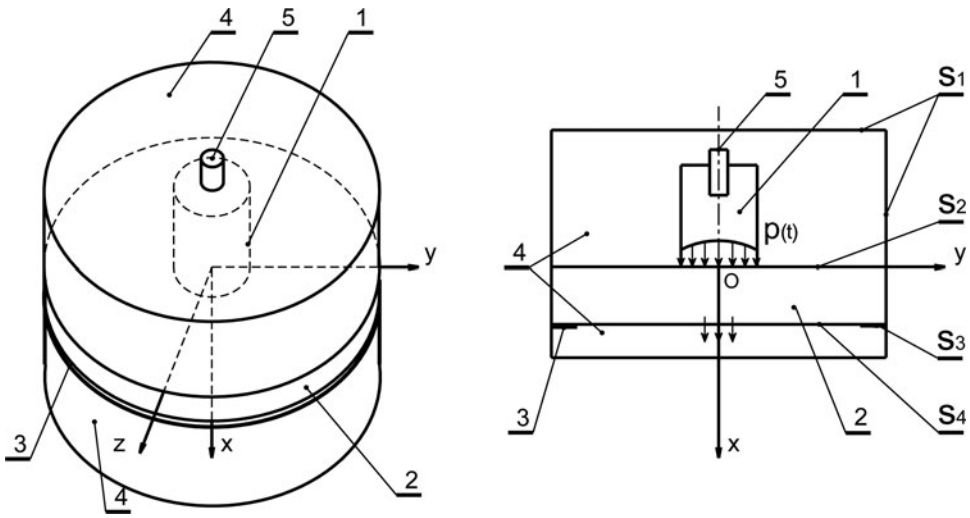

Figure 2. The physical model of the problem. 1: explosive; 2: steel plate; 3: shelf; 4: air environment; 5: detonator.

a steel plate (2), which is cylindrical, has diameter Φ, and has thickness B.

For detonating, a detonator (4) is placed on the free side of the explosive charge. The entire explosive–steel plate structure is placed in the infinite air environment (3).

When the explosive explodes, the detonation wave hits the front of the plate, the compressive wave enters the metal sheet material, and the reflected wave enters the detonation product medium. Under the effect of compressive waves at high velocity, the material undergoes elastic deformation and plastic deformation, leading to the formation of a concave funnel on the front; this process can be considered as an adiabatic process with a large part of the deformation work transformed into heat, and the material is heated to high temperatures (hundreds of degree Celsius). When the compressive wave travels to the free surface, the rarefaction wave is formed and reversed into the metal material, which makes the backing material tensile. If the tensile stress σ_1 exceeds the limit of the tensile stress σ_P, the material is pulled off, producing a collapsing funnel at the back. Theoretical and empirical evidence suggests that if the energy density of the sheet is large enough, the collapsing funnel goes deep into the plate, meets with the concave funnel, and creates a hole [3], [28].

2.1. *The partial differential equations*

Some basic assumptions are as follows:

1. Explosive is homogeneous in chemical composition and physical properties.
   The metal sheet material is homogeneous, isotropic, durable, and compressed.
2. Gravity effects are ignored on materials when interacting and moving.

The partial differential equations describe propagation of explosive, motion, stress state, deformation state of the environment in Lagrange variable for axial symmetry case, which consist of mass conservation equations, momentum conservation equations, energy conservation equations, equations of relativity, equations for determining the mechanical nature of materials, equation of state and kinematics equations. The axis of symmetry is the x-axis, the dots represent the derivative, and the θ subscript is the symbol that is perpendicular to the oxy plane [7]. Equation (4) consists of 23 basic equations with 23 unknowns:

x, y: the two projection components of Euler coordinate vector in x, y axes;
v_x, v_y: the two projection components of velocity vector in x, y axes;
$\varepsilon_{xx}, \varepsilon_{yy}, \varepsilon_{\theta\theta}, \varepsilon_{xy}$: the four projection components of strain tensor;
$\sigma_{xx}, \sigma_{yy}, \sigma_{\theta\theta}, \sigma_{xy}$: the four projection components of stress tensor;
$S_{xx}, S_{yy}, S_{\theta\theta}, S_{xy}$: the four projection components of deviatoric stress tensor;
λ: scalar quantity;
ε_i: strain intensity;
σ_i: stress intensity;
e: specific internal energy;
p, ρ, V: pressure, density, volume, respectively.

$$
\begin{cases}
\rho = \frac{\rho_0 V_0}{V} \\
\rho \frac{\partial v_x}{\partial t} = \frac{\partial \sigma_{xx}}{\partial x} + \frac{\partial \sigma_{xy}}{\partial y} + \frac{\sigma_{xy}}{y} \\
\rho \frac{\partial v_y}{\partial t} = \frac{\partial \sigma_{xy}}{\partial x} + \frac{\partial \sigma_{yy}}{\partial y} + \frac{\sigma_{yy} - \sigma_{\theta\theta}}{y} \\
\sigma_{xx} = -p + S_{xx};\ \sigma_{yy} = -p + S_{yy} \\
\sigma_{\theta\theta} = -p + S_{\theta\theta};\ \sigma_{xy} = S_{xy} \\
\dot{\varepsilon}_{xx} = \frac{\partial \dot{x}}{\partial x};\ \dot{\varepsilon}_{yy} = \frac{\partial \dot{y}}{\partial y} \\
\dot{\varepsilon}_{\theta\theta} = \frac{\dot{y}}{y};\ \dot{\varepsilon}_{xy} = \frac{1}{2}\left[\frac{\partial \dot{x}}{\partial y} + \frac{\partial \dot{y}}{\partial x}\right]; \\
\dot{S}_{xx} + 2G\dot{\lambda}S_{xx} = 2G\left[\dot{\varepsilon}_{xx} - \frac{1}{3}\frac{\dot{V}}{V}\right] \\
\dot{S}_{yy} + 2G\dot{\lambda}S_{yy} = 2G\left[\dot{\varepsilon}_{yy} - \frac{1}{3}\frac{\dot{V}}{V}\right] \\
\dot{S}_{\theta\theta} + 2G\dot{\lambda}S_{\theta\theta} = 2G\left[\dot{\varepsilon}_{\theta\theta} - \frac{1}{3}\frac{\dot{V}}{V}\right] \\
\dot{S}_{xy} + 2G\dot{\lambda}S_{xy} = 2G\dot{\varepsilon}_{xy} \\
\dot{\lambda} = \frac{3}{2\sigma_i^2}(\sigma_{xx}\dot{\varepsilon}_{xx}^{(P)} + \sigma_{yy}\dot{\varepsilon}_{yy}^{(P)} + \sigma_{\theta\theta}\dot{\varepsilon}_{\theta\theta}^{(P)} + \sigma_{xy}\dot{\varepsilon}_{xy}^{(P)}) \\
\sigma_i = \Phi(\varepsilon_i, \dot{\varepsilon}_i, p, T, \ldots) \\
\dot{e} = \frac{1}{\rho}(\sigma_{xx}\dot{\varepsilon}_{xx} + \sigma_{yy}\dot{\varepsilon}_{yy} + \sigma_{\theta\theta}\dot{\varepsilon}_{\theta\theta} + \sigma_{xy}\dot{\varepsilon}_{xy}) \\
p = p(\rho, e) \\
u_x = u_x(X, Y, t) = x(X, Y, t) - X;\ u_y = u_y(X, Y, t) \\
\quad = y(X, Y, t) - Y \\
v_x = \frac{\partial u_x}{\partial t} = \dot{u}_x(X, Y, t);\ v_y = \frac{\partial u_y}{\partial t} = \dot{u}_y(X, Y, t)
\end{cases}
\quad . \quad (4)
$$

2.2. *Initial conditions*

At the initial time ($t = 0$), we suppose that the explosive and metal sheet materials are not affected by external forces and standing still. We have the following initial conditions:

- State in the explosive material:

$$
\begin{aligned}
v_x^{TN}(x_i, y_i, 0) &= v_y^{TN}(x_i, y_i, 0) = 0 \\
\rho^{TN}(x_i, y_i, 0) &= \rho_0^{TN} \\
p^{TN}(x_i, y_i, 0) &= p_0^{TN} \\
e^{TN}(x_i, y_i, 0) &= e_0^{TN} \\
\varepsilon^{TN}{}_{xx}(x_i, y_i, 0) &= \varepsilon^{TN}{}_{yy}(x_i, y_i, 0) = 0 \\
\varepsilon^{TN}{}_{\theta\theta}(x_i, y_i, 0) &= \varepsilon^{TN}{}_{xy}(x_i, y_i, 0) = 0 \\
\sigma^{TN}{}_{xx}(x_i, y_i, 0) &= \sigma^{TN}{}_{yy}(x_i, y_i, 0) = 0 \\
\sigma^{TN}{}_{\theta\theta}(x_i, y_i, 0) &= \sigma^{TN}{}_{xy}(x_i, y_i, 0) = 0
\end{aligned}
$$

- State in metal material:

$$
\begin{aligned}
v_x^{T}(x_i, y_i, 0) &= v_y^{T}(x_i, y_i, 0) = 0 \\
\rho^{T}(x_i, y_i, 0) &= \rho_0^{T} \\
p^{T}(x_i, y_i, 0) &= p_0^{T}
\end{aligned}
$$

$$e^T(x_i, y_i, 0) = e_0^T$$
$$\varepsilon^T{}_{xx}(x_i, y_i, 0) = \varepsilon^T{}_{yy}(x_i, y_i, 0) = 0$$
$$\varepsilon^T{}_{\theta\theta}(x_i, y_i, 0) = \varepsilon^T{}_{xy}(x_i, y_i, 0) = 0$$
$$\sigma^T{}_{xx}(x_i, y_i, 0) = \sigma^T{}_{yy}(x_i, y_i, 0) = 0$$
$$\sigma^T{}_{\theta\theta}(x_i, y_i, 0) = \sigma^T{}_{xy}(x_i, y_i, 0) = 0$$

- State in the air:

$$\upsilon_x^{KK}(x_i, y_i, 0) = \upsilon_y^{KK}(x_i, y_i, 0) = 0$$
$$\rho^{KK}(x_i, y_i, 0) = \rho_0^{KK}$$
$$p^{KK}(x_i, y_i, 0) = p_0^{KK}$$
$$e^{KK}(x_i, y_i, 0) = e_0^{KK}$$
$$\varepsilon^{KK}{}_{xx}(x_i, y_i, 0) = \varepsilon^{KK}{}_{yy}(x_i, y_i, 0) = 0$$
$$\varepsilon^{KK}{}_{\theta\theta}(x_i, y_i, 0) = \varepsilon^{KK}{}_{xy}(x_i, y_i, 0) = 0,$$

where ρ_0^{TN}, ρ_0^T,ρ_0^{KK} are the density, p_0^{TN}, p_0^T, p_0^{KK} are the pressure and e_0^{TN}, e_0^T, e_0^{KK} are the specific internal energy values of the explosive, metal sheet and air at the initial time, respectively.

2.3. *Boundary conditions*

Boundary conditions ensure continuity at the contact surface between materials and air ambient.

On the S_1 boundary: This is the boundary between the air and the void (no material – as defined by AUTODYN) that is needed to set the boundary conditions without reflection, which ensures the expansion of detonation products when encountering this border without reflection. This is an algorithm that saves computer memory and ensures exactly the results of the problem.

On the S_2, S_4 boundary: Set the velocity and stress boundary conditions.

- *Velocity boundary conditions:* At the same point on the boundary, the elements of the materials have the same velocity:

$$\upsilon_y \cdot n = \upsilon_n \cdot n,$$

where υ_y and υ_n are the velocities at the same point of the two contact surfaces.

- *Stress boundary conditions:* Elements of materials at a boundary point have the same stresses of absolute value but vice versa, according to Newton's third law:

$$(\sigma_{ijy} - \sigma_{ijn})n^j = 0,$$

where σ_{ijy} and σ_{ijn} are the stresses at the points on the contact surface that have the same coordinates but fall on two surfaces, respectively.

On the S_3 boundary: Set the displacements of the points on the S_3 boundary of the plate to be always zero:

$$u_i|_{S_3} = 0.$$

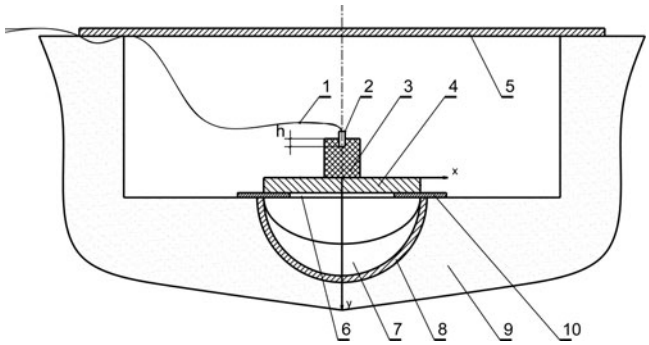

Figure 3. Empirical configuration. 1: power cable; 2: detonator; 3: explosive; 4: steel sample; 5: cover; 6: hole; 7: sand for collecting the fragments; 8: spherical pan; 9: soil; h: detonator's depth.

Movable boundary conditions for detonation products: Not that r is the radius of the detonation wave surface, which has a center at the point of detonating; u, p, and ρ are the speed, pressure, and density of the detonation products, respectively; D and t are the speed and time, respectively, of propagation of the detonation wave surface, we have the following:

- When $r = 0$, $u = 0$ and when $r = Dt$, $p = p_H$, $u = u_H$, $\rho = \rho_H$, where p_H, u_H, ρ_H are the parameters at Chapman–Jouguet point.
- When $t \geq r_0/D$ instead of the condition on the surface of the impact wave, new boundary conditions appear on the boundary of the detonation product – air.
- When $r = r_0$, $p = p_0^{KK}$, $\rho = \rho_0^{KK}$ (r_0 is the distance from the center of the explosion to the point of explosive-air) and when $r > r_0$, $p = p^{KK}$, $\rho = \rho^{KK}$.

3. Experimental setup

Based on the mathematical model, the empirical configuration is set up as shown in Figure 3.

Explosive specimen: Use C-4 explosives of a certain mass, cylindrical structure with different coefficients $\eta = L/d$ (L is charge height, d is the charge diameter). The chemical composition of C-4 explosive is shown in Table 1.

Steel specimen: Experimental steel samples are made from C45 rolled steel. Chemical composition is shown in Table 2, and some thermal properties of this steel can be seen in item 4.

Measuring equipment: An electronic Scout Pro 200 g scale of weighing range less than 200 g and precision 0.01 g.

After setting up the experimental configuration, we detonate the detonator and the explosive charge, destroy the steel plate, collect all of the fragments, and determine the mass on the Scout Pro 200 g scale.

Table 1. The chemical composition of C-4 explosive.

C-4 (%)	RDX (%)	Diethylhexyl sebacate (%)	Polyisobutylene (%)	Motor oil (%)
100	91	5.3	2.1	1.6

Table 2. The chemical composition of C45 steel.

C45 steel (%)	C (%)	Fe (%)	Mn (%)	P (%)	S (%)	Cu (%)	Si (%)	Others (%)
100	0.4491	98.43	0.6617	0.0175	0.0133	0.0052	0.2309	Balance

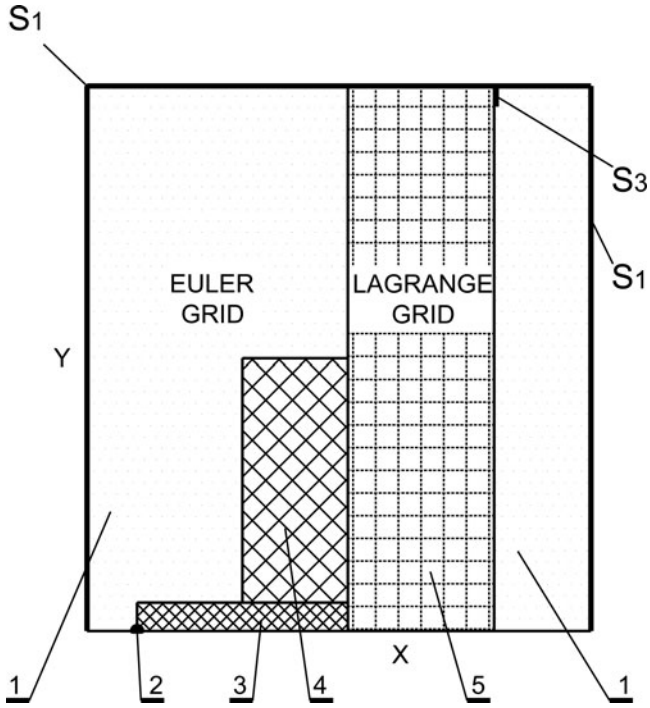

Figure 4. Schematic of the numerical model. 1: the air; 2: detonation point; 3: detonator; 4: explosive charge; 5: steel plate. S1: The boundary condition without reflection; S3: The boundary condition without move.

4. Setting up and solving problems with AUTODYN software

Because of the axial symmetry of the problem, we set up the problem in the AUTODYN-2D environment, having an axial symmetry as shown in Figure 4.

4.1. *Building object model*

Steel plate model: The steel plate is cylindrical, and the form of axial symmetry is rectangular in size (thickness × radius) = (10 mm × 45 mm). It is modeled in the Lagrange grid (Lagrange Solver option), and the grid size is (0.2 mm × 0.2 mm). The material parameters of the C45 steel are as follows: density $\rho_0 = 7870\,\text{kg/m}^3$; initial temperature $T_{ref} = 300\,\text{K}$; specific heat $C_V = 490$ J/kg K. The parameters in the shock equation of state are taken according to AISI 1006 steel in the AUTODYN's material library [18] (because C45 steel is an equivalent material to AISI 1006 steel): Gruneisen coefficient $\Gamma = 2.17$; sound speed $C_1 = 4569\,\text{m/s}$; coefficient $S_1 = 1.49$.

The parameters in the strength model of C45 steel are as follows [29], [30]:

- The von Mises strength model consists of shear modulus $G = 8.0 \times 10^7$ kPa and static yield stress $Y_s = 421$ MPa.
- The Johnson–Cook strength model consists of shear modulus $G = 8.0 \times 10^7$ kPa, melting temperature $T_{mel} = 8.11$ K, and the materials constants $A = 551$ MPa, $B = 608$ MPa, $C = 0.0134$, $n = 0.234$ and $m = 1$.

Failure criteria of the steel plate are the hydrodynamic tensile failure criteria; the failure pressure of C45 steel is $P_{\min} = -1.32$ GPa [29]. Use the *erosion/failure* option to remove elements once they meet the failure criteria.

The air model: In the form of axial symmetry, the air model is also rectangular, covering dimensions of C45 steel plate model and explosive charges. The air is modeled in the Euler mesh (Euler multimaterial solver option), mesh size (0.2 mm × 0.2 mm) with the ideal gas equation of state. Parameters of air materials are density $\rho_0 = 1.225\,\text{kg/m}^3$; adiabatic exponent $\gamma = 1.4$; initial temperature $T = 300$ K; and specific heat $C_V = 717.6$ J/kgK [17], [30].

The explosive charge model: The Fill option is used to insert explosive blocks into the air model. Such explosives also are modeled in the Euler grid with mesh size of 0.2 mm × 0.2 mm. Cylindrical explosive charges vary in size depending on the simulation cases, and the detonator is a Comp A-3 explosives cylinder (Φ3.5 mm × 18 mm) weighing 1.14 g. The parameters of explosive material are the following [3], [28]:

- *The Comp A-3 explosive material:* An RDX explosive is domesticated with density $\rho_0 = 1650\,\text{kg/m}^3$; Chapman–Jouguet pressure $P_{CJ} = 3.0 \times 10^7$ kPa; detonation velocity $D = 8300\,\text{m/s}$. The JWL equation of state includes the following experimental coefficients: $A = 611.3$ GPa; $B = 10.65$ GPa; $R_1 = 4.4$; $R_2 = 1.2$; $W = 0.32$; $E_{CJ} = 8.9 \times 10^6\,\text{kJ/m}^3$.
- *The C-4 explosive model:* The model has Density $\rho_0 = 1601\text{kg/m}^3$; Chapman–Jouguet pressure $P_{CJ} = 2.8 \times 10^7$ kPa; detonation velocity $D = 8193\,\text{m/s}$. The JWL equation of state includes the experimental coefficients: $A = 609.8$ GPa; $B = 12.95$ GPa; $R_1 = 4.5$; $R_2 = 1.4$; $W = 0.25$; $E_{CJ} = 9.0 \times 10^6\,\text{kJ/m}^3$.

4.2. *Setting initial conditions*

The initial conditions of the material (initial density, pressure, etc.) are declared by the user.

4.3. *Setting boundary conditions*

The boundary condition without reflection S_1: The flow-out boundary is set up and assigned to the boundary S_1.

The boundary condition without move S_3: The horizontal velocity of constant ($v_x = 0$) is set up and assigned to the boundary S_3. The boundary conditions of detonation products-explosive and detonation products-air automatically perform when computed in the Euler multimaterial solver. The boundary conditions S_2 and S_4 are automatically implemented by the Euler–Lagrange couple algorithm.

4.4. *Setting interactive controls*

Setting Lagrange–Lagrange interactive control: The *Calculate* button is clicked to calculate the interactive distance for the Lagrange grids together.

Setting Euler–Lagrange interactive controls: The *Automatic (Polygon free)* button is clicked to calculate the interactive distance for the Lagrange grid and Euler grid.

4.5. *Setting detonation control*

We choose the detonation type *Point* in the *Detonation* tab and enter the coordinates of the detonation point in the free head (on the *ox* axis) of the Comp A-3 explosive block.

Table 3. Experimental constants for the Johnson–Cook model and von Mises model of C45 steel.

TT	Experimental constants	Johnson–Cook model	von Mises model
1	A (MPa)	551	—
2	B (MPa)	608	—
3	Harding coefficient, C	0.0134	—
4	Harding exponent, n	0.234	—
5	Softening exponent, m	1	—
6	Static yield strength, Y_s (MPa)	—	421

After setting the stop condition in the *Control* tab, the output variable controls in the *Output* tab, button *Start* is clicked to begin solving the problem.

5. Results and discussion

5.1. *Features of the sequence of errors when using two different strength models*

As described above, for using the Johnson–Cook strength model, five empirical constants have to be determined. For using the von Mises model, only one experimental parameter is required (Table 3).

In order to solve the destruction problem, failure criteria should be determined empirically. For destruction problems of metal sheet, both theoretical and empirical evidence suggests that using the hydrodynamic tensile failure criteria (P_{min}) is appropriate.

However, the empirical determination of P_{min} for materials at high deformation rates is not possible in a number of laboratories. Works nowadays can reference the value P_{min} according to the documents of the similar material and allow changing this value within a certain range to obtain the required precision.

Problem using the Johnson–Cook strength model may face large errors when it has to take all six experimental constants according to literature (A, B, C, n, m, and P_{min}), while problem using the von Mises strength model just takes two constants (Y_s and P_{min}). In order to select an appropriate strength model, the authors carry out numerical simulations of both Johnson–Cook and von Mises strength models for C45 steel, 10 mm thick, C-4 explosive 20 g. Cylindrical explosive charge has a different

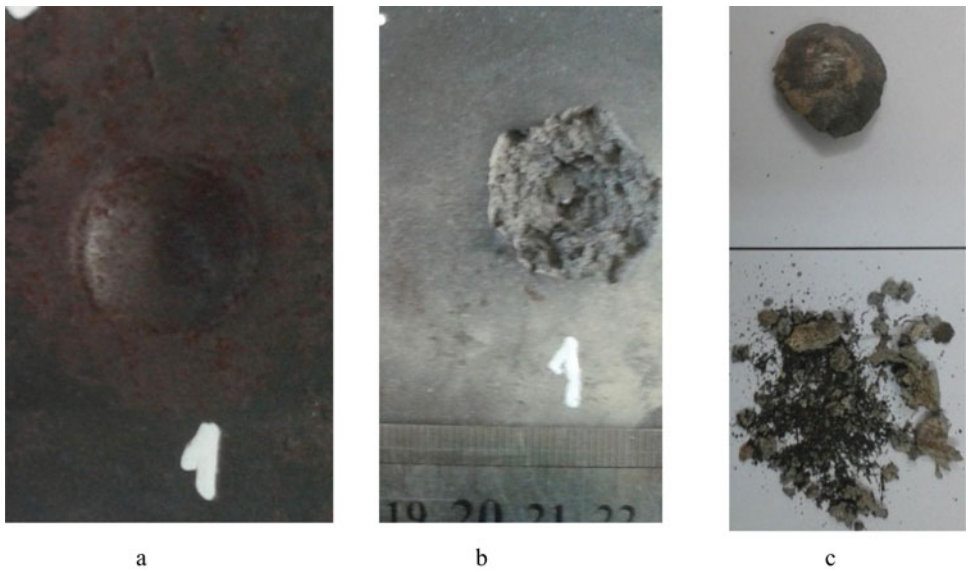

Figure 5. Destruction and fragmentation results, $\eta = 2.0$. (a) Concave funnel. (b) Collapsing funnel. (c) Fragments.

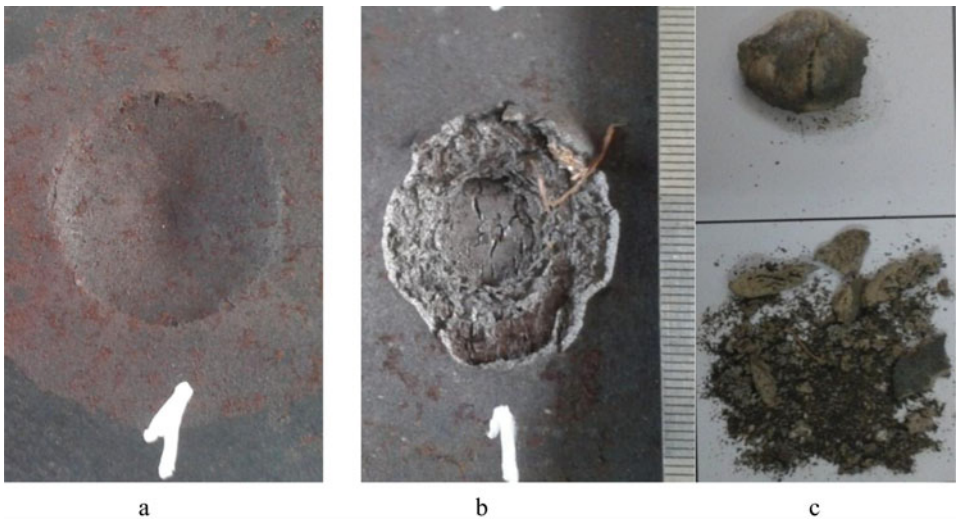

Figure 6. Destruction and fragmentation results, $\eta = 1.5$. (a) Concave funnel. (b) Collapsing funnel. (c) Fragments.

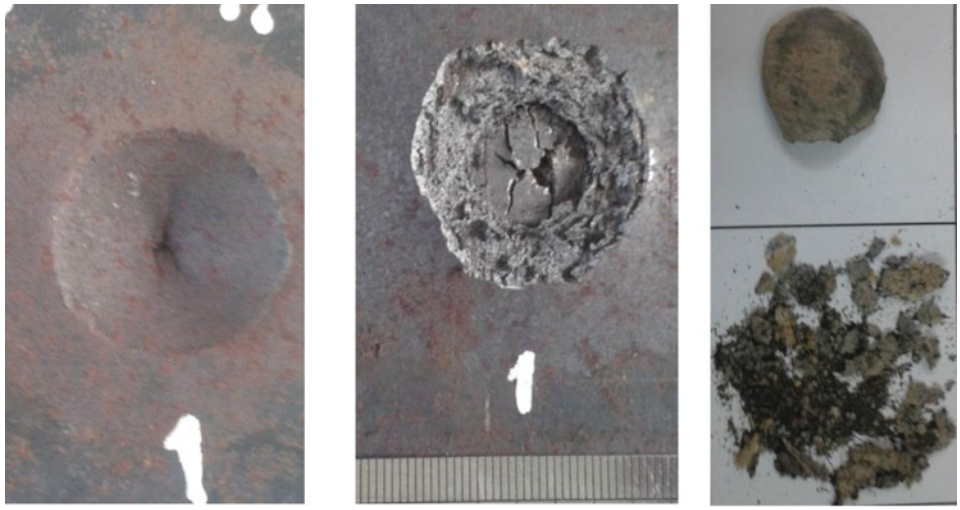

Figure 7. Destruction and fragmentation results, $\eta = 1.0$. (a) Concave funnel. (b) Collapsing funnel. (c) Fragments.

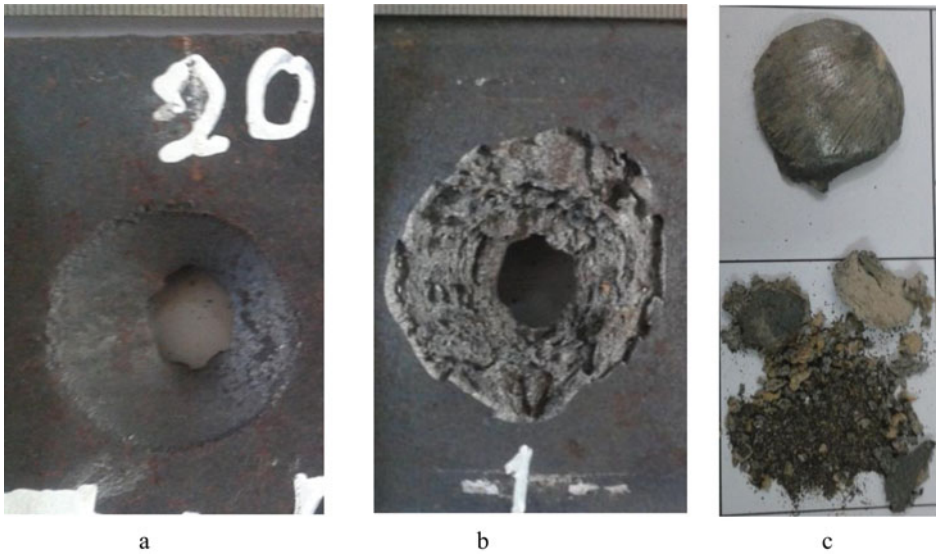

Figure 8. Destruction and fragmentation results, $\eta = 0.5$. (a) Concave funnel. (b) Collapsing funnel. (c) Fragments.

structural coefficient η. Simulation results were compared with empirical results.

First, we observe the experimental results, the images of the destroyed surfaces of the C45 sheet (concave funnel, collapsing funnel), and the total mass of fragments (destruction mass) with different values of η clearly shown.

When keeping the explosive mass C-4 (20 g) and changing the value of η to 2.0, 1.5, 1.0 and 0.5, the size of the destroyed surface and the destruction mass increased sharply (Figures 5–8 and Table 4).

Figure 9 shows the suitability between the size of the destruction surface, the size of the holes in the numerical simulations, and the experiment at $\eta = 0.5$. The diameter of experimental hole is 13 mm, while the diameters of holes in the numerical simulations are 16.5 mm (using the Johnson–Cook model) and 14.3 mm (using the von Mises model).

Table 4. Calculated and experimental destruction mass for C45 steel of 10 mm thickness.

	Charge						Destruction mass (g)				
								Johnson–Cook		von Mises	
Order	Mass (g)	η	L (mm)	d (mm)	h (mm)	Thick-ness of steel sheet (mm)	Exp. value	Value	Error to exp. (%)	Value	Error to exp. (%)
1	20	2.0	40.4	20.2	12	10	9.41	5.4	− 42.7	7.4	− 21.4
2	20	1.5	33.4	22.2	12	10	14.1	7.5	− 47.6	12.4	− 12.1
3	20	1.0	25.4	25.4	12	10	16.6	10.4	− 37.6	13.4	− 20.0
4	20	0.5	16	32	12	10	29.65	30.6	2.5	25.5	− 14.0

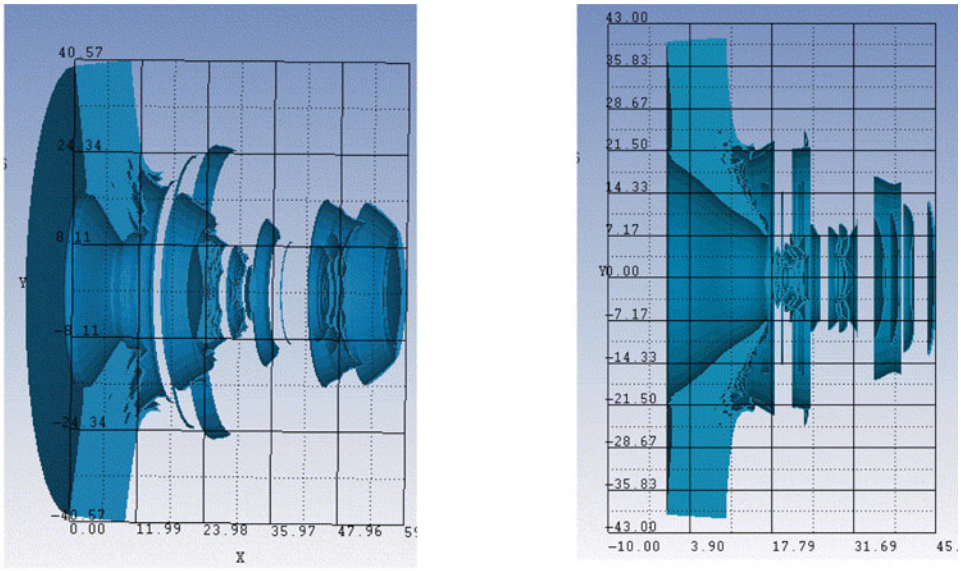

a b

Figure 9. Simulation results for 20 g C-4, $\eta = 0.5$. (a) Using the Johnson–Cook model. (b) Using the von Mises model.

Based on Table 4, this paper analyzed the data of two sequences of errors from the numerical simulations using the Johnson–Cook and von Mises models versus the same experiments. The range R is calculated for the two sequences of errors using the following formula:

$$R = x_{max} - x_{min}. \tag{5}$$

We have

$$R_{J-C,\eta} = -42.7 - 2.5 = -45.2(\%),$$
$$R_{V-M,\eta} = -21.4 - (-12.1) = -9.3(\%).$$

We see that the range of the sequence of errors using von Mises model is very small compared to that using the Johnson–Cook model. The variance s^2 and the standard deviation $s$of the two errors sequences are calculated according to the following formula [19]:

$$s^2 = \frac{\sum_{i=1}^{n} (x_i - \bar{x})^2}{n-1}. \tag{6}$$

We have

$$s^2_{J-C,\eta} = 525.9;\ s_{J-C,\eta} = 22.9(\%),$$
$$s^2_{V-M,\eta} = 20.4;\ s_{V-M,\eta} = 4.5(\%).$$

Thus, when keeping the explosive mass C-4 (20 g) and the thickness of the steel plate, and changing the structural coefficient η, the sequence of errors using the von Mises strength model that includes range, variance and standard deviation is much lower compared to that of errors using the Johnson–Cook strength model.

5.2. *Determination of the standard deviation of entire sets using two strength models*

To determine the standard deviation of entire sets using the two strength models, experiments and numerical simulations are carried out for two 8-mm and 12-mm steel plates. In each plate thickness, we changed the explosive mass and structural coefficient η; the results are recorded in Table 5.

Using all of the data in Tables 4 and 5, we calculated the range, variances and standard deviations of the sequence of errors, which take into account the variation of the structural coefficient η, the thickness of the plate B, and explosive mass ω; the results are shown in Table 6.

According to Table 6, range, variances, and standard deviations of error sequence computed by using the von Mises strength model are much smaller compared to those using the Johnson–Cook strength model. We use the Chi-square test to perform a variance inference for the entire set of errors when

Table 5. Calculated and experimental destruction mass for two C45 steel sheet plates of 8 mm and 12 mm thickness, respectively.

	Explosive charge						Destruction mass (g)				
								Johnson–Cook		von Mises	
Order	Mass (g)	η	L (mm)	d (mm)	h (mm)	Thick-ness of steel sheet (mm)	Exp. value	Value	Error to exp. (%)	Value	Error to exp. (%)
1	16	1.0	23.7	23.7	12	12	14.06	18.5	31.5	13.5	− 4.2
2	16	0.5	15	30	12	12	26.60	33.6	25.8	24.5	− 8.0
3	12	1.0	21.7	21.7	12	8	8.11	6.3	− 22.2	8.31	2.2
4	14	0.75	18.5	25.2	12	8	14.93	11.2	− 25.2	13.2	− 11.8

Table 6. Statistical values for error sequences when computed according to different strength models.

		According to the Johnson–Cook model		According to the von Mises model	
Order	Statistical values	Notation	Value	Notation	Value
1	Range, R (%)	R_{J-C} (%)	78.9	R_{V-M} (%)	23.6
2	Variances, S^2(%^{2})	S^2_{J-C}(%^{2})	345.1	S^2_{V-M}(%^{2})	27.4
3	Standard deviations, S(%)	S_{J-C}(%)	18.6	S_{V-M}(%)	5.2

Table 7. The standard deviation (σ) of entire sets.

Strength model	Null hypothesis, H_0	Alternative hypothesis, H_1	Degree of freedom, df	Chi-square, χ^2	p value	Outcome
von Mises	$\sigma_{V-M} = 9.4(\%)$	$\sigma_{V-M} < 9.4(\%)$	7	2.14	0.048	$\sigma_{V-M} < 9.4(\%)$
Johnson–Cook	$\sigma_{J-C} = 33.8(\%)$	$\sigma_{J-C} < 33.8(\%)$	7	2.12	0.047	$\sigma_{J-C} < 33.8(\%)$

computed in these two models with a 95% confidence interval (α level is 0.05) and degree of freedom (df) equal to 7 (sample size, $n = 8$) [31], [32]. The results are shown in Table 7; the standard deviation of the entire set simulated by the von Mises model is less than 9.4%, while the standard deviation computed using the Johnson—Cook model is less than 33.8%. Thus, the value of standard deviation using the von Mises model is fulfilling the error requirement in the study.

6. Conclusion

After constructing the mathematical model, the authors set up the destruction problem of metal plate by contact explosive charge in highly nonlinear dynamics software AUTODYN and solved the problem in two cases using the Johnson–Cook strength model (with five material constants A, B, C, n, m, and failure critical P_{min}, all were taken according to literature) and using the von Mises strength model (with the static yield stress Y_s, that has to be determined in a simple tension test, and unique failure critical, which was taken according to literature). The numerical simulation results were compared with the experimental results and showed the good fit of numerical calculations versus experimental results. Statistical calculations have shown important conclusions:

1. When the thickness of the steel plate and explosive mass are constant, if we change the structural coefficient η, the sequence of errors using the von Mises strength model, which has range, variance and standard deviation, is much lower compared to the sequence of errors using the Johnson–Cook strength model.
2. With the 95% confidence, the standard deviation of the entire set of errors using the von Mises strength model is less than 9.4%, while the standard deviation of the entire set of errors using the Johnson–Cook model is less than 33.8%. Thus, the value of standard deviation for the von Mises model is satisfactory for the error in the study.

The conclusions drawn have important theoretical and practical meanings. A new approach has been opened up in the study for the destruction of steel plates by contacting explosive charge in particular, by high speed impact in general for a lot of metallic materials having mechanical properties, such as C45 steel, because the unique static yield stress is required to save research costs. The results of the study also show that the Johnson–Cook strength model, if used inappropriately, would result in large errors; this helps to avoid mistakes in the next high speed impact study.

Funding

This research is funded by Vietnam National University, Hanoi under Grant number QG.17.45. The authors are grateful for this support.

References

[1] V. Aune, G. Valsamos, F. Casadei, M. Langseth, and T. Borvik, "On the dynamic response of blast-loaded steel plates with and without pre-formed holes," *Int. J. Impact Eng.*, vol. 108, pp. 27–46, 2017. DOI:10.1016/j.ijimpeng.2017.04.001.

[2] G. Heilig, N. Durr, M. Sauer, and A. Klomfass, "Mesoscale analysis of sintered metals fragmentation under explosive and subsequent impact loading," *Proc. Eng.*, vol. 58, pp. 653–662, 2013. DOI:10.1016/j.proeng.2013.05.075.

[3] F. A. Baum and L. P. Orlenko, *Physics Explosion*. Moscow: Fizmatlit, 2002.

[4] P. Ludwik, *Elemente der Technologischen Mechanik*. Berlin: Julius Springer, 1909.

[5] J. H. Hollomon, "Tensile deformation," *Trans. AIME*, vol. 162, pp. 268–290, 1945.

[6] H. W. Swift, "Plastic instability under plane stress," *J. Mech. Phys. Solids*, vol. 1, pp. 1–18, 1952. DOI:10.1016/0022-5096(52)90002-1.

[7] ANSYS, Inc., *AUTODYN®Explicit Software for Nonlinear Dynamice, Theory Manual Revision 4.3*. Concord: Century Dynamics, Inc., 2005.

[8] J. O. Hallquist, *LS-DYNA Theoretical Manual*. California: Livermore Software Technology Corporation, 1988.

[9] J. O. Hallquist, *LS-DYNA Theoretical Manual*. California: Livermore Software Technology Corporation, 2006.

[10] G. R. Johnson and W. H. Cook, "Fracture characteristics of three metals subjected to various strains, strain rates, temperatures and pressures," *Eng. Fract. Mech.*, vol. 21, pp. 31–48, 1985. DOI:10.1016/0013-7944(85)90052-9.

[11] D. Forni, B. Chiaia, and E. Cadoni, "Strain rate behaviour in tension of S355 steel: Base for progressive collapse analysis," *Eng. Struct.*, vol. 119, pp. 164–173, 2016. Doi:10.1016/j.engstruct.2016.04.013.

[12] R. L. Azevedo and M. Alves, "A numerical investigation on the visco-plastic response of structures to different pulse loading shapes," *Eng. Struct.*, vol. 30, pp. 258–267, 2008. DOI:10.1016/j.engstruct.2007.04.002.

[13] D.-N. Zhang, Q.-Q. Shangguan, C.-J. Xie, and F. Liu, "A modified Johnson–Cook model of dynamic tensile behaviors for 7075-T6 aluminum alloy," *J. Alloys Compd.*, vol. 619, pp. 186–194, 2015. DOI:10.1016/j.jallcom.2014.09.002.

[14] A. E. Buzyurkina, I. L. Gladkyb, and E. I. Krausa, "Determination and verification of Johnson–Cook model parameters at high-speed deformation of titanium alloys," *Aerosp. Sci. Technol.*, vol. 45, pp. 121–127, 2015. DOI:10.1016/j.ast.2015.05.001.

[15] O. Rezaifar, M. Z. Kabir, M. Taribakhsh, and A. Tehranian, "Dynamic behaviour of 3D-panel single-storey system using shaking table testing," *J. Eng. Struct.*, vol. 30, pp. 318–337, 2008. DOI:10.1016/j.engstruct.2007.03.019.

[16] M. H. Abedini-Sanigy, F. Ahmadi, E. Goshtasbirad, and M. Yaghoubi, "Thermal stress analysis of absorber tube for a parabolic collector under quasi-steady state condition," *Energy Proc.*, vol. 69, pp. 3–13, 2015. DOI:10.1016/j.egypro.2015.03.002.

[17] R. Frans, H. Parung, D. Sandy, and S. Tonapa, "Numerical modeling of hexagonal castellated beam under monotonic loading," *Proc. Eng.*, vol. 171, pp. 781–788, 2017. DOI:10.1016/j.proeng.2017.01.449.

[18] ANSYS, Inc., ANSYS 14.0 Help, 2011.

[19] N. D. Duc, N. D. Tuan, T. Phuong, T. Q. Quan, and N. V. Quyen, "Nonlinear dynamic response of imperfect FGM plates subjected to blast load," in *Proc. XII Natl. Conf. Mech. Deformed Solid*, 2015, vol. 1, pp. 472–479.

[20] N. D. Duc, N. D. Tuan, and T. Q. Quan, "Analytical approach for investigating the nonlinear dynamic response of imperfect shear deformable FGM cylindrical panel subjected to blast loads," in *Proc. 14th East Asia-Pacific Conf. Struct. Eng. Constr. (EASEC14)*, 2016, pp. 218–219.

[21] C. Qi, S. Yang, L. J. Yang, S. H. Han, and Z. H. Lu, "Dynamic response and optimal design of curved metallic sandwich panels under blast loading," *Sci. World J.*, vol. 2014, pp. 1–14, 2014. DOI:10.1155/2014/853681.

[22] S. Li, X. Li, Z. Wang, G. Wu, G. Lu, and L. Zhao, "Finite element analysis of sandwich panels with stepwise graded aluminum honeycomb cores under blast loading," *Int. J. Mech. Sci.*, vol. 96–97, pp. 1–12, 2015. DOI:10.1016/j.ijmecsci.2015.03.011.

[23] N. D. Duc, N. D. Tuan, T. Phuong, and T. Q. Quan, "Nonlinear dynamic response and vibration of imperfect shear deformable functionally graded plates subjected to blast and thermal loads," *J. Mech. Adv. Mater. Struct.*, vol. 24, pp. 318–329, 2017. DOI:10.1080/15376494.2016.1142024.

[24] N. D. Duc and P. H. Cong, "Nonlinear dynamic response and vibration of sandwich composite plates with negative Poisson's ratio in auxetic honeycombs," *J. Sandwich Struct. Mater.*, pp. 1–26, 2016. DOI: 10.1177/1099636216674729.

[25] N. T. Duong and N. D. Duc, "Evaluation of elastic properties and thermal expansion coefficient of composites reinforced by randomly distributed spherical particles with negative Poisson's ratios," *J. Compos. Struct.*, vol. 153, pp. 569–577, 2016. DOI:10.1016/j.compstruct.2016.06.069.

[26] G. Imbalzano, T. Phuong, N. D. Tuan, and V. S. L. Perter, "A numerical study of auxetic composite panels under blast loadings," *Compos. Struct.*, vol. 135, pp. 339–352, 2016. DOI:10.1016/j.compstruct.2015.09.038.

[27] N. D. Duc, K. Seung-Eock, P. H. Cong, N. T. Anh, and N. D. Khoa, "Dynamic response and vibration of composite double curved shallow shells with negative Poisson's ratio in auxetic honeycombs core layer on elastic foundations subjected to blast and damping loads," *Int. J. Mech. Sci.*, vol. 133, pp. 504–512, 2017. DOI:10.1016/j.ijmecsci.2017.09.009.

[28] M. L. Wilkins. "Calculation of elastic-plastic flow," *Methods Comput. Phys.*, vol. 3, pp. 211–263, 1964.

[29] T. Antoun, *Spall Fracture*. New York: Springer, 2003.

[30] G. G. Ye, *et al.*, "Cutting AISI 1045 steel at very high speeds," *Int. J. Mach. Tools Manuf.*, vol. 56, pp. 1–9, 2012. DOI:10.1016/j.ijmachtools.2011.12.009.

[31] S. F. Arnold, *Mathematical Statistics*. USA: Prentice-Hall, 1990.

[32] P. Mathew, *Design of Experiments with Minitab*. USA: ASQ Quality Press, 2005.